

Fiber Longitudinal Monitoring of Inter-band-SRS-induced Power Transition in S+C+L WDM Transmission

Runa Kaneko, Takeo Sasai, Fukutaro Hamaoka, Masanori Nakamura, and Etsushi Yamazaki

NTT Network Innovation Laboratories, 1-1 Hikari-no-oka, Yokosuka, Kanagawa, 239-0847 Japan
runa.kaneko@ntt.com

Abstract: We experimentally demonstrate the fiber-longitudinal power profile estimation (PPE) over the S+C+L band, which captures power transition in the propagation direction due to inter-band stimulated Raman scattering only using receiver-side signal processing. © 2024 The Author(s)

1. Introduction

The ultra-wideband (UWB) wavelength division multiplexing (WDM) transmission beyond the traditional C band is required meet the continuous growth in data traffic demand [1]. However, in the UWB transmission over S+C+L band, the signal power transition due to the inter-band stimulated Raman scattering (SRS) becomes significant, which affects the total transmission capacity [2]. The success of such UWB systems largely depends on monitoring and management of both spectral and spatial power profile to ensure sufficiently high OSNR and low fiber Kerr nonlinearity across all channels. Recently, there have been extensive studies on fiber longitudinal power profile estimation (PPE) [3–7], which can extract multi-span spatial power profile by processing received signals at a coherent receiver. This monitoring solution does not require additional optical configuration and dedicated equipment like OTDR, thereby reducing CAPEX/OPEX of network monitoring. By performing PPE using multiple channels, the spectral power profile monitoring has been demonstrated for C band [3] and C+L band [4].

In this paper, we present and experimentally demonstrate fiber-longitudinal monitoring of inter-band-SRS-induced power transition in 12.9-THz S+C+L UWB WDM transmission. We show that, by performing PPE using multiple WDM channels, both spectral and spatial power profiles of the entire transmission link over S+C+L band can be obtained. As a result, monitoring of spatial power reduction in S band and increase in the L band due to inter-band SRS power transition as well as the resulting spectral tilt at any positions can be achieved. The demonstration indicates that the PPE can be used to facilitate performance prediction and power management of UWB systems in the presence of inter-band SRS.

2. Power Profile Estimation

In this work, we applied a PPE method described in [5] to monitor the power transition attributed to the inter-band SRS. PPE estimates the power evolution in the fiber's longitudinal direction from the received signal using only Rx DSP. To this end, PPE uses fiber nonlinear phase rotation to estimate power profiles, leveraging their proportionality. In fact, the power profile of the transmission link appears as $\gamma'(z)$ in the generalized nonlinear Schrödinger equation: $\frac{\partial A}{\partial z} = j \frac{\beta_2}{2} \frac{\partial^2}{\partial z^2} A - j \gamma'(z) |A|^2 A$, where $\gamma'(z) \equiv \gamma(z)P(z) = \gamma(z)P(0) \exp(-\int_0^z \alpha(z') dz')$ and β_2 , $\gamma(z)$, $P(z)$, and $\alpha(z)$ are the group velocity dispersion, nonlinear coefficient, signal power profile, and fiber loss, respectively, and $A = A(z, t)$ is the optical signal at position z and time t with power normalized to unity. The least-squares-based PPE [3,5,7], estimates $\gamma'(z)$ as the optimal value such that the square error between the received signal from the actual transmission link and that from the emulated link is minimized.

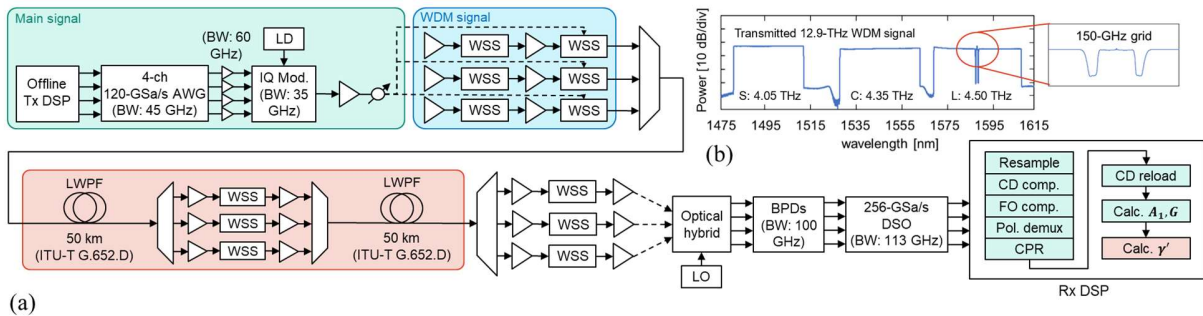


Fig. 1. (a) Schematic diagram of experimental setup in S+C+L-band WDM transmission and (b) optical spectrum of transmission WDM signal.

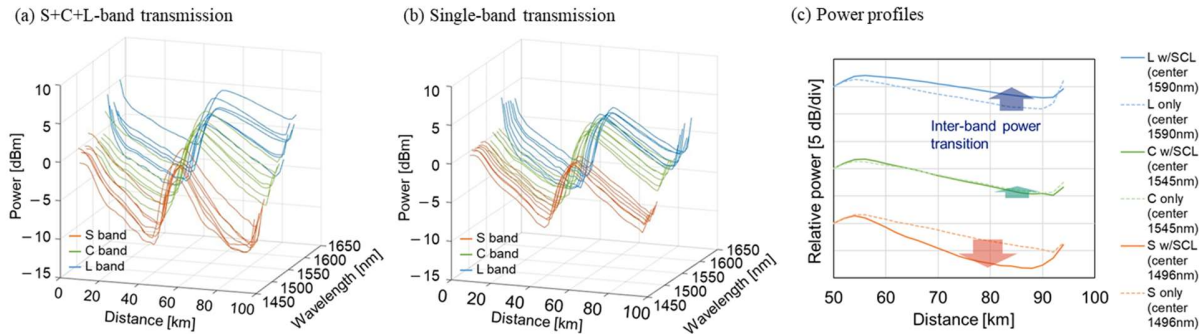


Fig. 2. Estimated power profiles of each wavelength in (a) S+C+L-band transmission and (b) single-band transmission, and (c) Power profile comparison of S+C+L-band and single-band transmission in the second span.

PPE measures the power evolution of the channel under test at a specific wavelength. By applying PPE across multiple WDM channels, we can reconstruct the spectral power profile. Particularly in the presence of inter-band SRS, S-band channels experience a reduction in power, whereas L-band channels observe a power increase. These channels undergo excessively low or high Kerr nonlinearity depending on their power, and thus PPE can capture power transition due to inter-band SRS. Importantly, PPE can be conducted using data-carrying signals without the need for special training pilot signals or sequences. This indicates that this monitoring solution works in actual system operation.

3. Experimental Setup

The experimental setup is shown in Fig. 1 (a). The main signal is generated by a transmitter consisting of a 4-ch 120-GSa/s arbitrary waveform generator (AWG), an IQ modulator, and laser diodes (LDs), and PCS 64QAM ($H = 4.347$, $IR = 3.305$, 21% FEC OH) 100 GBaud with a roll-off factor of 0.1. The WDM signals in the S, C, and extended L bands are emulated using amplified spontaneous emission light sources, and spectral flattening is performed by a wavelength selective switch (WSS). The main signal and WDM channels are multiplexed and transmitted through a 50-km \times 2-span low water peak fiber (LWPF) link, which complies with ITU-T G.652. D. For amplification, signals are temporarily demultiplexed to each band and amplified by EDFA and TDFA with spectral shaping using WSS. On the receiving side, the main signal is filtered by the WSS. The receiver consists of a 90° optical hybrid, local oscillators (LOs), balanced photodetectors (BPDs), and a 256-GSa/s digital storage oscilloscope (DSO). In Rx DSP, equalization processes are performed, such as resampling, chromatic dispersion compensation, frequency offset compensation, polarization demultiplexing, carrier phase recovery, and chromatic dispersion reloading. LLS-PPE is then performed to estimate $\gamma'(z)$.

Fig. 1 (b) shows the transmitted signal spectrum over S+C+L band with a total bandwidth of 12.9-THz. The fiber input powers in the S, C, and extended L bands are 17.66, 19.15, and 19.21 dBm with 28, 30, and 31 channels, respectively. The utilized bandwidths are 1481.19–1511.43 nm in the S band, 1528.77–1563.45 nm in the C band, and 1570.83–1608.76 nm in the extended L band. For each band, we conducted the LLS-PPE at equally spaced 7 channels. The wavelength-dependency of γ is corrected on the basis of [8]. 20 power profiles are averaged and a moving average of 5 points are also performed to suppress fluctuations in the estimated power profiles.

4. Results and Discussion

Fig. 2 (a) and (b) shows the estimated power profiles for the S+C+L-band and the single-band transmission scenarios. Note that, in Fig. 2 (b), all the profiles in S, C, and L bands are simultaneously shown although PPE was performed under the single-band transmission scenario. In Fig. 2(a), the power in the S band decreased compared to the other bands while the power in the L band increased toward the end of the transmission span. On the other hand, in Fig. 2 (b), there tends to be less power transition during single band transmission. These results show that PPE can capture the power transitions occurred due to inter-band SRS in the S+C+L-band transmission scenario. Fig. 2 (c) shows the power profiles of the center wavelength in each band, and this more clearly represents the power transition. The longitudinal power variation in S band and L band was successfully observed while there was almost no change in the power profiles at the center frequency of C band, possibly indicating that the inter-band SRS from S and L bands balanced.

Fig. 3 (a) shows the optical spectrum estimated by PPE over the S, C, and L band at the 80 km point during S+C+L-band transmission. The solid line is the reference spectrum observed by an optical spectrum analyzer (OSA) placed at 80 km, and the dotted line is the one at the input of the second span. The significant power transition from shorter

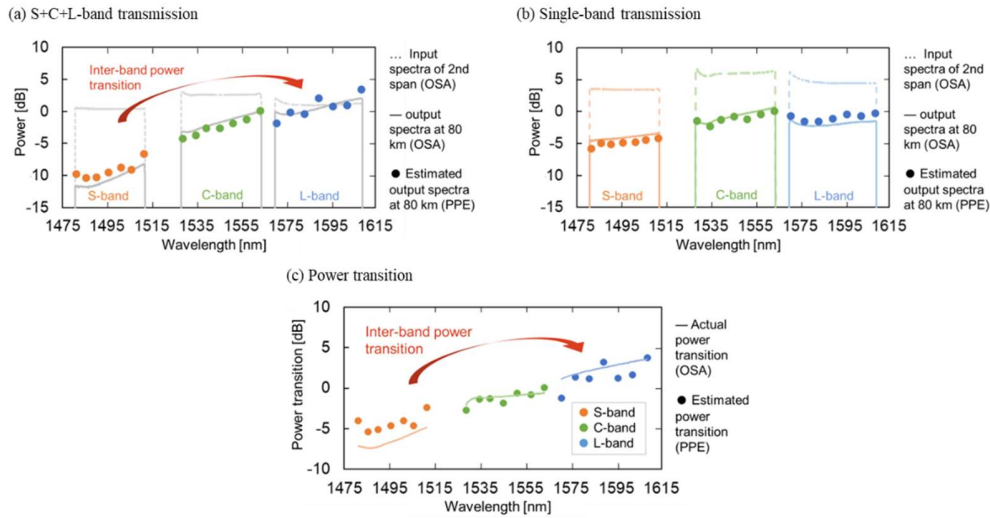


Fig. 3. The optical power spectra of (a) S+C+L-band transmission, (b) single-band transmission, and (c) the power transition suggesting inter-band SRS.

wavelengths to longer wavelengths was observed. The spectrum obtained by PPE also captures the spectral tilt due to the inter-band ISRS. To quantify the accuracy of the spectrum obtained by PPE, we use $RMSE = \sqrt{\frac{1}{K} \sum_{k=0}^{K-1} |P_k^{PPE} - P_k^{OSA}|^2}$, where P_k is power level of the spectrum at wavelength k . The RMSE of spectra for S+C+L-band transmission was 1.36 dB in the S band, 0.69 dB in the C band, 1.10 dB in the L band, and 1.09 dB in all bands. The accuracy of PPE at S band was worst compared to other bands. This is because the power in the S band during S+C+L-band transmission becomes small due to the inter-band SRS, and the resulting PPE also becomes instable due to insufficient Kerr nonlinearity, as can be seen from Fig. 2. Fig. 3 (b) shows the spectra of each band during the single band transmission. The slope of the spectrum is smaller compared to that of Fig. 3 (a), indicating that inter-band SRS had almost disappeared, but a slight amount of intra-band SRS had remained. The RMSE for the single-band transmission was 0.84 dB in the S band, 0.50 dB in the C band, 1.00 dB in the L band, and 0.81 dB in all bands. Focusing on the S band, the estimation accuracy improved due to the reduction in power transitions. Fig. 3 (c) shows the amount of power transition which was determined by subtracting the spectrum for single band transmission from the one for S+C+L-band transmission. The amount of power transition calculated by PPE shows the same tendency as that calculated by OSA. The RMSE was 2.17 dB in the S band, 0.49 dB in the C band, 1.34 dB in the L band, and 1.50 dB in all bands. The spectrum obtained from PPE also captures trends in excess loss in the S band and Raman gain in the L band.

5. Conclusion

In this paper, we demonstrated longitudinal monitoring of the power transition caused by inter-band SRS in the S+C+L UWDM transmission. This is achieved by applying the longitudinal power profile estimation, which can reveal the distance- and wavelength-dependent power profile and the optical spectrum at any distance. This technique is expected to facilitate the performance prediction and management of UWDM systems that are becoming more complex due to the power transition due to the inter-band SRS.

6. References

- [1] F. Hamaoka, *et al.*, "173.7-Tb/s Triple-Band WDM Transmission using 124-Channel 144-GBaud Signals with SE of 9.33 b/s/Hz," OFC, Th3F.2 (2023).
- [2] B. Feng, *et al.*, "Performance Evaluation of S+C+L-Band Optical Transmission over G.652.D and G.654.E Fibers," CLEO, JW3B.105 (2022).
- [3] T. Sasai, *et al.*, "Digital Longitudinal Monitoring of Optical Fiber Communication Link," J. Lightw. Technol., 40 (8), 2390 (2022).
- [4] M. Sena, *et al.*, "DSP-Based Link Tomography for Amplifier Gain Estimation and Anomaly Detection in C+L-Band Systems," J. Lightw. Technol., 40 (11), 3395 (2022).
- [5] T. Sasai, *et al.*, "Linear Least Squares Estimation of Fiber-Longitudinal Optical Power Profile" J. Lightw. Technol., early access (2023).
- [6] T. Tanimura, *et al.*, "Experimental demonstration of a coherent receiver that visualizes longitudinal signal power profile over multiple spans out of its incoming signal," ECOC (2019).
- [7] I. Kim, *et al.*, "Longitudinal Power Profile Estimation in WDM Transmission and Optical Network Tomography," OECC (2023).
- [8] P. Poggiolini, *et al.*, "Closed Form Expressions of the Nonlinear Interference for UWDM Systems," ECOC, Tu1D.1 (2022).